Analysis of Dielectric-Loaded Cavities for Characterization of the Nonlinear Properties of High Temperature Superconductors

J. Mateu, C. Collado, O. Menéndez, and J. M. O'Callaghan

Abstract—**This work describes and compares two alternative methods of analyzing dielectric-loaded cavities for measurement of intermodulation distortion in HTS films. One of them is based on assuming a specific type of HTS nonlinearities and developing theoretical equations based on them. The second is based on a numerical approach that can be applied to many types of nonlinearities. Both methods are shown to work on measured data of representative HTS films.**

Index Terms—**Dielectric cavities, high temperature superconductors, intermodulation, nonlinearities.**

I. INTRODUCTION

MICROWAVE nonlinearities, and particularly intermodulation distortion, are a potential obstacle in the development of analog applications of High Temperature Superconductors (HTS). The experimental characterization of intermodulation distortion (IMD) is mostly based on the measurement of patterned planar resonators [1], [2]. In these resonators there are high current densities near the pattern edges and there is concern that this, together with the possible film damage at the pattern edges, might be a cause of misleading results in the measurements. To circumvent this, we have recently proposed to do intermodulation measurements with a TE_{011} rutile-loaded cavity resonator similar to the ones used for surface resistance measurement, and we have derived equations that relate the intermodulation products to the properties of the HTS films for some specific cases of HTS nonlinearities [3]. In this work we present an alternative approach of analyzing the cavity based on its nonlinear equivalent circuit, which can be efficiently treated by using numerical methods of nonlinear circuit analysis. This approach has the advantage of not being restricted to a specific type of HTS nonlinearities. Also, for the specific cases of HTS nonlinearity for which an analytical solution exists, the numerical approach is not subject to some simplifying assumptions which restrict the range of validity of the analytical solution.

J. Mateu is with CTTC-Centre Tecnològic de Telecomunicacions de Catalunya. Edifci NEXUS. 08034-Barcelona, Spain.

C. Collado, O. Menéndez, and J.M. O'Callaghan are with Universitat Politècnica de Catalunya (UPC), Campus Nord UPC D3. Barcelona, Spain 08034 (e-mail: joano@tsc.upc.es).

II. FORMULATION OF HTS NONLINEARITIES

We assume that, if the current density at the surface of a superconductor is high enough, the superconductor will produce an electric field $\overrightarrow{e_{NL}}$ that will be superimposed to the one due to the linear surface impedance of the material. We further assume that this field depends on the surface current j_s and has a (nonlinear) resistive and reactive term, [4]:

$$\overrightarrow{e_{NL}}(j_s) = a_{NL}(j_s)\overrightarrow{j_s} + \frac{\partial}{\partial t}\left[b_{NL}(j_s)\overrightarrow{j_s}\right] \qquad (1)$$

where $\overrightarrow{j_s}$ is the surface current density, $a_{NL}(j_s)$ the nonlinear resistive term and $b_{NL}(j_s)$ the nonlinear reactive one. Both terms depend on the magnitude of the surface current j_s and have to be zero for $j_s = 0$ since $\overrightarrow{e_{NL}}$ is negligible if j_s is small. We have used (1) in several previous works about modeling of HTS nonlinearities [3], [5]. In the analysis made in this work, we restrict $a_{NL}(j_s)$ and $b_{NL}(j_s)$ to $a_{NL}(j_s) = \Delta R_\alpha |j_s|^\alpha$, $b_{NL}(j_s) = \Delta L_\alpha |j_s|^\alpha$ where α, ΔR_α, ΔL_α are parameters that characterize the strength of the nonlinearity in the HTS. As detailed in [3], with this formulation one can match the experimental slope of the power of the intermodulation products versus the power of the fundamental signals thought the parameter α, and ΔR_α, ΔL_α set how much of the nonlinearity can be attributed to the resistive or the reactive part of (1). With these restrictions, (1) reads:

$$\overrightarrow{e_{NL}} = \Delta R_\alpha |j_s|^\alpha \overrightarrow{j_s} + \Delta L_\alpha \frac{d}{dt}\left(|j_s|^\alpha \overrightarrow{j_s}\right). \qquad (2)$$

III. CAVITY ANALYSIS

The TE_{011} cavity used (Fig. 1) is similar to the ones used for surface resistance (R_s) measurements of HTS films [6], [7]. However, unlike in R_s measurements, one of the endplates in our cavity may be a normal metal since it is not required that the HTS losses dominate the overall cavity loss. This has the advantage of making the nonlinear properties of the cavity dependent on the nonlinearities of a single HTS film at the expense of reducing the circulating power and the power of the intermodulation products. Another difference from typical cavities used for R_s measurements is that we prefer using one-port cavities. This allows us to make intermodulation measurements with a setup in which, if the cavity is critically coupled, the fundamental tones
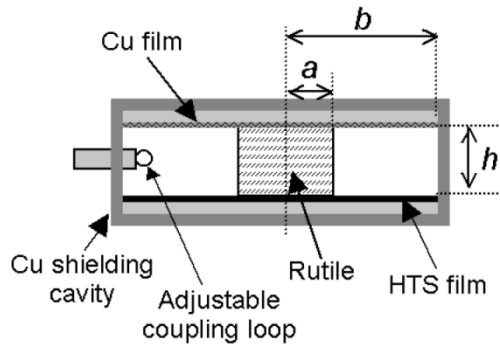
Fig. 1. Schematic diagram of the rutile-loaded cavity. One of the endplates is a normal metal and the other a HTS film. This arrangement can be used for characterizing nonlinearities in 10 mm $\times$ 10 mm HTS films.

coming out of the cavity do not mask the intermodulation products [3].

A. Electric Field on the HTS Film

In an intermodulation experiment, where signals at ω_1 and ω_2 are injected to the cavity, the surface current density on the HTS film at ω_1 and ω_2 is:

$$\vec{j}_s(\rho, t) = (j_1 \cos \omega_1 t + j_2 \cos \omega_2 t) f(\rho) \hat{\phi} \qquad (3)$$

where $f(\rho)$ is the radial dependence of the surface current of the TE_{011} mode, i.e., [7]:

$$f(\rho) = \begin{cases} \frac{\beta}{\xi_1} J_1(\xi_1 \rho) & \rho \le a \\ \frac{\beta}{\xi_2} \frac{J_0(\xi_1 a)}{F_0(\xi_2 a)} F_1(\xi_2 \rho) & a < \rho < b \end{cases} \qquad (4)$$

where β is the z-direction propagation constant, ξ_1 and ξ_2 are the ρ-direction wavenumbers (inside and outside the dielectric respectively), $F_0(\xi_2 \rho) = I_0(\xi_2 \rho) + K_0(\xi_2 \rho) I_1(\xi_2 a) / K_1(\xi_2 a)$, $F_1(\xi_2 \rho) = -I_1(\xi_2 \rho) + K_1(\xi_2 \rho) I_1(\xi_2 a) / K_1(\xi_2 a)$ being $J_0, J_1, I_1, I_2, K_0, K_1$, the corresponding Bessel and Hankel functions.

The electric field on the HTS film $\vec{e_{NL}}$ can be found using (3) and (4) in (2):

$$\vec{e_{NL}}(\rho, t) = \{\Delta R_\alpha |A(t)|^\alpha A(t)$$
$$+ \Delta L_\alpha \frac{d}{dt} (|A(t)|^\alpha A(t))\} |f(\rho)|^\alpha f(\rho) \hat{\phi} \quad (5)$$

where $A(t) = (j_1 \cos \omega_1 t + j_2 \cos \omega_2 t)$. Note that this is the product of a time-varying function and another one describing the spatial dependence of $\vec{e_{NL}}$. Thus, the electric field at the intermodulation frequency will be of the form

$$\vec{E}_{2\omega_1 - \omega_2} = E_{2\omega_1 - \omega_2} |f(\rho)|^\alpha f(\rho) \hat{\phi} \qquad (6)$$

with

$$E_{2\omega_1 - \omega_2} = [\Delta R_\alpha + j(2\omega_1 - \omega_2) \Delta L_\alpha] 2C_{2\omega_1 - \omega_2} \qquad (7)$$

and

$$C_{2\omega_1 - \omega_2} = \lim_{T \to \infty} \frac{1}{T} \int_{-T/2}^{T/2} |A(t)|^\alpha A(t) e^{-j(2\omega_1 - \omega_2)t} dt. \quad (8)$$

where $C_{2\omega_1 - \omega_2}$ depends only on j_1, j_2 and α.

B. IMD Power Coupled Out of the Resonator

The electric field generated on the HTS surface at frequency equal to $2\omega_1 - \omega_2$ will launch a resonant TE_{011} mode in the cavity whose amplitude will depend on the loaded $Q(Q_L)$ at $2\omega_1 - \omega_2$. The magnetic field of this mode on the HTS surface has to have the same radial dependence as $\vec{j}_s$ in (3) and thus its phasor has to follow:

$$\vec{H}_{2\omega_1 - \omega_2} = H_{2\omega_1 - \omega_2} f(\rho) \hat{\rho}. \qquad (9)$$

The next step in the analysis is to find $H_{2\omega_1 - \omega_2}$. This can be done by finding the power generated at $2\omega_1 - \omega_2$ on the HTS surface through a surface integral of $\vec{E}_{2\omega_1 - \omega_2} \times \vec{H}^*_{2\omega_1 - \omega_2}$ and making it equal to the power that is dissipated in the cavity or coupled out of it [3]. Using (6) and (9) this results in:

$$\frac{1}{2} E_{2\omega_1 - \omega_2} H^*_{2\omega_1 - \omega_2} \int_S |f(\rho)|^\alpha f(\rho) f(\rho) dS$$
$$= \frac{(2\omega_1 - \omega_2) W_0}{Q_L} H^*_{2\omega_1 - \omega_2} H_{2\omega_1 - \omega_2} \quad (10)$$

where $W_0 |H_{2\omega_1 - \omega_2}|^2$ is the total energy stored in the resonator at $2\omega_1 - \omega_2$. From (7), (8) and (10) we can find $H_{2\omega_1 - \omega_2}$ as a function of the nonlinear parameters of the film (ΔR_α, ΔL_α, α), the amplitude of the surface currents (j_1, j_2), the normalized field distribution of the TE_{011} mode ($W_0, f(\rho)$) and the Q_L of the cavity:

$$H_{2\omega_1 - \omega_2} = [\Delta R_\alpha + j(2\omega_1 - \omega_2) \Delta L_\alpha]$$
$$\cdot 2C_{2\omega_1 - \omega_2} \frac{Q_L}{(2\omega_1 - \omega_2) W_0} \Gamma_\alpha \qquad (11)$$

where $\Gamma_\alpha = (1/2) \int_S |f(\rho)|^\alpha f(\rho) f(\rho) dS$.

The power coupled out of the cavity at $2\omega_1 - \omega_2$ (P_L) is the coupling factor (κ) times the power dissipated in the cavity, i.e.,:

$$P_L = \kappa \frac{(2\omega_1 - \omega_2) W_0}{Q_0} |H_{2\omega_1 - \omega_2}|^2 \qquad (12)$$

where Q_0 is the unloaded quality factor of the cavity.

Finally, using (12), (11) and (8) one could calculate this power if the amplitudes of the surface current density (j_1, j_2) were known. To find them, it is convenient to relate these amplitudes with the available power of the sources at ω_1 and ω_2 (P_{0,ω_1} and P_{0,ω_2}). This can be done by relating the power dissipated in the cavity ($\omega_1 W_0 j_1^2 / Q_0$ for ω_1) with the available power and the coupling factor κ:

$$\frac{4\kappa P_{0,\omega_1}}{(1 + \kappa)^2} \frac{1}{1 + Q_L^2 \Delta^2(\omega_1)} = \frac{\omega_1 W_0}{Q_0} j_1^2. \qquad (13)$$

where ω_0 is the resonant frequency and $\Delta(\omega_1) = 1 - \omega_0^2 / \omega_1^2$ takes into account the frequency response of the resonator, i.e., takes into account the fact that ω_1 does not coincide with the resonant frequency ω_0 [8]. The value of j_1 can be determined from (13) (an equivalent equation can be used for j_2).

C. Limitations of the Analysis

The procedure described above makes several implicit assumptions:

1) Only the mixing of fields at ω_1 and ω_2 is producing intermodulation fields at $2\omega_1 - \omega_2$. This neglects, for example, the third order mixing of the spurious at $3\omega_2 - 2\omega_1$ with the fundamental signal at ω_2 to produce a spurious at $2\omega_1 - \omega_2$.

2) It is assumed that the amplitudes of the currents j_1, j_2 are the same as they would be in a linear regime (see (13)). This neglects the fact that losses at ω_1 and ω_2 may increase as power is increased, and also neglects the power that is transferred from ω_1 and ω_2 to the frequencies of the spurious signals. This assumption will not be valid at very high powers.

3) We are forcing the nonlinear resistive part (first term in (2)) to have the same power dependence as the nonlinear reactive one (second term in (2)). We could overcome this by repeating the analysis with minor modifications to allow for different α's to be used in each part.

4) We are restricting $a_{NL}(j_s)$ and $b_{NL}(j_s)$ in (1) to be proportional to $|j_s|^\alpha$ (see(2)).

The restrictions imposed by these assumptions are avoided with the procedure described in the following section.

IV. NUMERICAL PROCEDURE FOR IMD CALCULATIONS

The equivalent circuit of the cavity is shown in Fig. 2, where the source producing the sinusoidal signals at ω_1 and ω_2 is modeled as a current source with a shunt impedance Z_s (typically $50\,\Omega$), coupling is modeled as a transformer, and a transmission line is used to model the axial propagation in the cavity. As discussed in Section IV.B, the linear behavior of the two endplates is modeled as the line's terminating impedances and the nonlinearity of the HTS is modeled by a one-port whose voltage V_{nl} has a nonlinear dependence with the current across it (I_1).

A. Equivalents Between Fields, Voltages and Currents

The currents and voltages in the line are taken to be proportional to the transverse magnetic and electric fields in the waveguide. Following the steps in [9], we write the transverse fields $(\vec{H}_t, \vec{E}_t)$ in a forward-propagating TE_{01} wave in the dielectric waveguide as:

$$\vec{H}^+_t = \frac{I^+}{C_2} f(\rho)e^{-j\beta z}\widehat{\rho} \tag{14}$$

$$\vec{E}^+_t = Z_{TE_{01}} \frac{V^+}{C_1} f(\rho)e^{-j\beta z}\widehat{\phi} \tag{15}$$

where V^+, I^+ are the voltage and current of the forward-propagating wave in the transmission line and C_1, C_2 are proportionality constants (having dimensions of $\Omega\cdot m$ and m respectively). To determine C_1, C_2, we make the characteristic impedance in the transmission line equal to the impedance of the TE_{01} mode in the waveguide, thus from (14), (15) C_1/C_2 has to be equal to
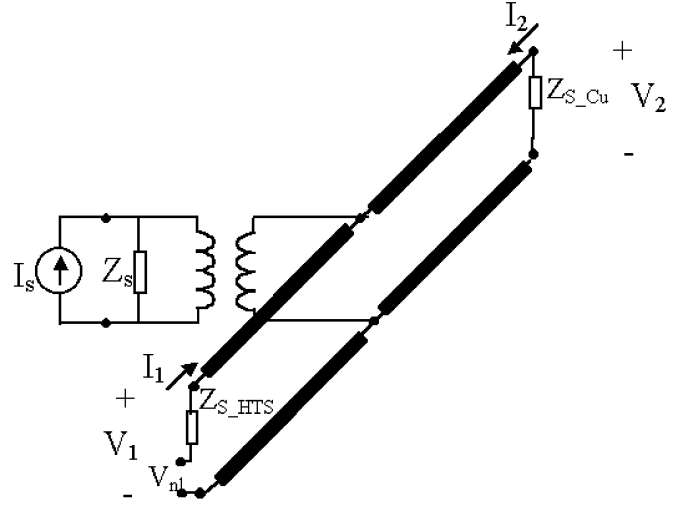

Fig. 2. Equivalent circuit of the cavity. The transmission line models the axial propagation in the cavity. The line's terminating impedances are equal to the surface impedance of the endplates in the cavity. The nonlinearity of the HTS is modeled as a linear one-port series with its surface resistance.

V^+/I^+ which is the characteristic impedance of the line which we are choosing to be $Z_{TE_{01}}$, i.e.,:

$$\frac{C_1}{C_2} = Z_{TE_{01}}. \tag{16}$$

The second condition used to determine C_1, C_2 is to match the power flow in the transmission line ($(1/2)V^+I^{+*}$) with that of the waveguide, which can be calculated with a surface integral of $\vec{E}^+_t \times \vec{H}^{+*}_t$. This results in:

$$C_1 = \frac{\omega\mu}{\xi_1}\sqrt{2\pi\left(IJ2 + \left(\frac{\xi_1}{\xi_2}\right)^2\left|\frac{J_0(\xi_1 a)}{F_0(\xi_2 a)}\right|^2 IF2\right)} \tag{17}$$

where $IJ2 = \int_0^a |J_1(\xi_1\rho)|^2\,\rho d\rho$ and $IF2 = \int_a^b |F_1(\xi_1\rho)|^2\,\rho d\rho$.

B. Terminations and Iterative Procedure

It follows from (14)–(17) that, if the waveguide is terminated by an endplate having a surface impedance Z_s, the transmission line in the equivalent circuit should also be terminated by a lumped impedance of identical value. With this we can account for the linear behavior of the endplates in the equivalent circuit of Fig. 2.

Taking into account the nonlinearities in one of the endplates is somewhat more involved, and is very closely related to the way the circuit is analyzed. We first neglect the nonlinearities and analyze the equivalent circuit (with $V_{nl} = 0$) to find the total current in the termination in frequency domain (I_1). With this current, and with the equivalence between fields and currents of the previous section, we find the time domain current distribution on the endplate $\vec{j}_s(\rho, t)$ which, as in (3), has a radial dependence given by $f(\rho)$. Equation (1) is then used to find the time-domain electric field on the HTS surface $\vec{e}_{NL}$. Next,
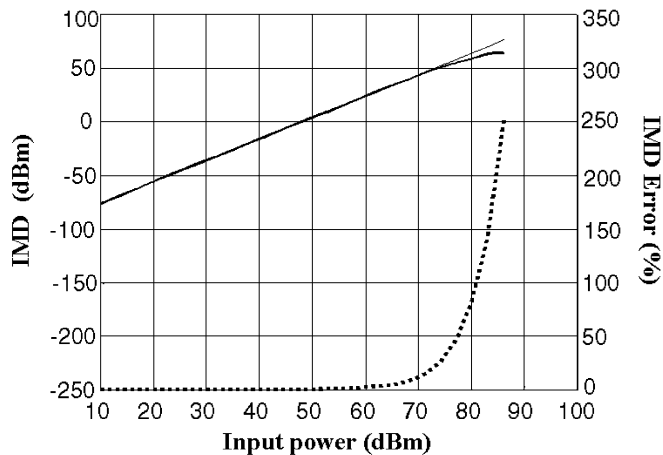
Fig. 3. Calculated power of the intermodulation products using the analytical and numerical approach for YBCO on MgO (solid lines, left scale) and IMD error between the two methods (dashed line, right scale). Unlike the results coming from the analysis (straight line), the ones obtained with the numerical method show compression effects, but these occur at unrealistically high power levels.

we convert this field back to frequency domain and find the amplitudes of the TE_{01} modes at each frequency (ω_1, ω_2 and all the spurious generated by the nonlinearity in (1)). These mode amplitudes determine a voltage in the equivalent circuit (V_{nl}) which can be calculated through the equivalence between fields and voltages of the previous section. This voltage, together with the current source I_s, affects all voltages and currents in the equivalent circuit, including I_1. Therefore, an iterative refinement of the solution can be done by analyzing the linear response of the circuit to I_s and the current estimate of V_{nl}, obtaining I_1 from this estimate, and using I_1 to find the nonlinear response of the HTS endplate and an updated value of V_{nl}. This iterative procedure is an adapted version of the Harmonic Balance algorithm that we have used in previous works related to HTS microwave nonlinearities [10].

V. RESULTS

Close agreement between the analytical and numerical approach has been obtained for a wide range of HTS nonlinear parameters (ΔR_α, ΔL_α, α). The comparison we present here is made with parameters obtained from measurements of a commercial 700 nm YBa$_2$Cu$_3$O$_{7-\delta}$ (YBCO) film grown on MgO [3]: $\alpha = 1$, $\Delta L_\alpha = 3.5 \times 10^{-16}$ Hm/A, $\Delta R_\alpha = 0$. With these parameters, the discrepancies between the analytical and numerical values of the power of the intermodulation products are of the order of 1% at low powers. This is attributed to quantization errors in the numerical calculation. Our data shows that the discrepancies tend to increase sharply at higher powers, but this occurs at an unrealistically high source power (Fig. 3). At these

high powers, thermal effects and not (1) should be expected to be dominant in the nonlinear behavior of the cavity.

We have looked in the literature for other IMD measurements of unpatterned films from which to extract nonlinear parameters and compare them with the ones above, to confirm that our method is working with representative data. This can be done in the disk resonator measurements presented in [11], for which our analysis in [5] showed that they are consistent with a characteristic current density j_{IMD} of 5.2×10^{12} A/m^2. A similar analysis with the value of ΔL_α above yields a j_{IMD} of 1.8×10^{12} A/m^2 and thus, the nonlinear properties of the films involved are reasonably similar.

VI. CONCLUSION

We have developed a technique to calculate intermodulation distortion in resonators with HTS materials for a specific type of HTS nonlinearities in which the resistive and/or reactive non-linearities scale with current density as $|j_s|^\alpha$. We have applied this technique to a rutile resonator to use it for characterization of unpatterned 10 mm $\times$ 10 mm HTS films. An alternative numerical approach has been also been developed and tested, and may be used in the future in other films whose nonlinearities do not follow a dependence with $|j_s|^\alpha$.

REFERENCES

[1] B. A. Willemsen, T. Dahm, and D. J. Scalapino, "Microwave intermodulation in thin film high-tc superconducting microstrip hairpin resonators: Experiment and theory," *Appl. Phys. Lett.*, vol. 71, no. 29, p. 3898, 1997.

[2] D. E. Oates, A. C. Anderson, D. M. Sheen, and S. M. Ali, "Stripline resonator measurements of zs versus hrf in ybacuo thin films," *IEEE Trans. Microwave Theory Tech.*, vol. 39, no. 9, p. 1522, 1991.

[3] J. Mateu, C. Collado, O. Menéndez, and J. M. O'Callaghan, Experiments and Model of Intermodulation Distortion in a Rutile Resonator with YBACUO Endplates, submitted for publication.

[4] J. Mateu, C. Collado, and J. M. O'Callaghan, "Nonlinear analysis of disk resonators. Application to material characterization and filter design," *IEEE Trans. Appl. Supercond.*, vol. 11, no. 1, pp. 135–138, 2001.

[5] C. Collado, J. Mateu, T. J. Shaw, and J. O'Callaghan, "HTS nonlinearities in microwave disk resonators," Physica C, to be published.

[6] N. Klein, C. Zuccaro, U. Dähne, H. Schulz, and N. Tellmann, "Dielectric properties of rutile and its use in high temperature superconducting resonators," *J. Appl. Phys.*, vol. 78, no. 11, pp. 6683–6686, 1995.

[7] J. Mazierska and R. Grabovickic, "Circulating power, rf magnetic field, and current density of shielded dielectric resonators for power handling analysis of high-temperature superconducting thin films of arbitrary thickness," *IEEE Trans. Appl. Supercond.*, vol. 8, no. 4, p. 178, 1998.

[8] M. J. Lancaster, *Passive Microwave Device Applications of High-Temperature Superconductors*. Cambridge, U.K.: Cambridge Univ. Press, 1997.

[9] D. M. Pozar, *Microwave Engineering*. New York: Wiley, 1998, ch. 4, pp. 83–87.

[10] C. Collado, J. Mateu, and J. M. O'Callaghan, "Nonlinear simulation and characterization of devices with HTS transmission lines using harmonic balance algorithms," *IEEE Trans. Appl. Supercond.*, vol. 11, no. 1, pp. 1396–1399, 2001.

[11] S. Kolesov, H. Chaloupka, A. Baumfalk, and T. Kaiser, "Planar HTS structures for high power applications in communications systems," *J. Supercond.*, vol. 10, no. 3, p. 179, 1997.